

ABSTRACT

**Title of Thesis: VISUALIZATION OF CERAMIDE CHANNEL
BY TRANSMISSION ELECTRON
MICROSCOPY**

Soumya Samanta, Master of Science, 2011

**Thesis directed by: Professor Marco Colombini
Department of Biology**

Functional studies have shown that the sphingolipid ceramide, self-assembles in phospholipid membranes to form large channels capable of allowing proteins to cross the membrane. Here these channels are visualized by negative stain transmission electron microscopy. The images contain features consistent with stain-filled pores having a roughly circular profile. There is no indication of tilt, and the results are consistent with the formation of right cylinders. The sizes of the pores range from 5 to 40 nm in diameter with an asymmetric distribution indicating no apparent upper size limit. The size distribution matches well with the distribution of sizes calculated from electrophysiological measurements.

VISUALIZATION OF CERAMIDE CHANNELS BY TRANSMISSION ELECTRON MICROSCOPY

By

Soumya Samanta

Thesis submitted to the Faculty of the Graduate School of the
University of Maryland, College Park, in partial fulfillment
of the requirements for the degree of
Master of Science

2011

Advisory Committee:

Professor Marco Colombini, Chair

Professor Ibrahim Ades

Professor Sergei Sukharev

© Copyright by

Soumya Samanta

2011

Acknowledgements

I would like to thank my advisor Professor Marco Colombini for his guidance, encouragement and support. Dr. Colombini introduced me to new experimental techniques, and always had time for my questions. He also helped me to think critically about my project at times and gave me ideas that shaped this project. I would like to thank Timothy Maugel, in charge of the Laboratory of Ultrastructure located at Biology/ Psychology building, University of Maryland at College Park for providing me with necessary training in transmission electron microscopy, and letting me use the facility whenever I needed it. I want to thank Dr. Ibrahim Ades and Dr. Sergei Sukharev for serving on my committee. Also, I would like to thank both Pamela Brock and Lois Reid for being so kind and having so much patience with all of my questions.

I want to thank my fellow graduate students of my lab, Vidyaramanan Ganesan, and Meenu N Perera and Shang Hsuan Lin for all of their help. Finally, I would like to take this opportunity to thank my friends and family for their kind support during my graduate school days. Especially my heartiest thanks go to my parents. Without their support, I would not have achieved my career goal.

TABLE OF CONTENTS

List of Figures.....	IV
List of Abbreviations	V
Chapter 1: Introduction.....	1-21
Chapter 2: Materials and Methods.....	22-27
Chapter 3: Results & Discussion.....	28-36
Chapter 4: Conclusion	37
Bibliography.....	38-41

LIST OF FIGURES

Figure.1. Schematic diagram of mitochondria mediated apoptosis pathway.....	2
Figure.2. Structure of ceramide molecule.....	6
Figure.3. Schematic diagram of <i>de novo</i> ceramide synthesis.....	9
Figure.4. Schematic diagram of sphingomyelinase transport pathway.....	10
Figure.5. Functionally derived structure of ceramide channel.....	11
Figure .6. A Schematic diagram of transmission electron microscope.....	16
Figure.7. Cartoon of a liposome with a channel.....	23
Figure.8. Location of liposomes with channel and without channel in density gradient centrifugation.....	29
Figure.9. Liposomes with ceramide treatment having channels.....	30
Figure.10. Liposomes with control vehicle treatment.....	31
Figure.11. Histogram of channel diameters.....	32
Figure.12. Plot profile of a ceramide channel.....	33
Figure.13. Expected tilt of channel edge compared to experimental data	34
Figure. 14. Comparison of ceramide channel size distribution (TEM Vs. Elecphys)	35

LIST OF ABBREVIATION

C₁₆-ceramide: *N*-palmitoyl-*D*-erythro-sphingosine

MOM: Mitochondrial Outer Membrane

PTP: Permeability Transition Pore

MAC: Mitochondrial Apoptosis-induced Channel

TEM: Transmission Electron Microscopy

VDAC: Voltage Dependent Anion Channel

NAIP: Neuronal Apoptosis Inhibition Factor

TNF: Tumor Necrosis Factor

APAF: Apoptosis Protease Activating Factor

AIF: Apoptosis Inducing Factor

SMAC: Second Mitochondria-derived Activator of Caspases

DIABLO: Direct IAP-Binding protein with Low pI

Chapter 1: INTRODUCTION

Apoptosis (a form of programmed cell death) is an intracellular, multi-step mechanism of shedding unwanted cells from the body. There is a specific biochemical paradigm involved with each step of apoptosis. There are two different pathways through which programmed cell death can take place:

1. Extrinsic
2. Intrinsic

Surface receptors play a very important role in the cellular signaling processes, namely Fas and Tumor Necrosis Factor (TNF) are primarily responsible for the initiation of extrinsic apoptosis. Fas-Fas ligand mediated and TNF-receptor (TNFR) (1, 2) mediated models are two accepted models of the extrinsic pathway of apoptosis. Apart from these two models, another TNF dependent model is TRAIL (TNF-Related Apoptosis-Inducing Ligand) (3).

The intrinsic pathway involves mitochondria to a great extent. It also involves caspases and Bcl-2 family proteins. Upon an apoptotic insult, i.e. oxidative stress, DNA damage, mitochondrial disturbances etc, the Mitochondrial Outer Membrane (MOM) becomes permeable to various Inter Membrane Space (IMS) proteins such as cytochrome *c* and Smac/DIABLO. These proteins are released into the cytosol, which starts the onset of the execution phase of apoptosis by participating in the cascade pathway.

There are some common hallmark characteristics of an apoptotic cell irrespective of the pathway through which it is executed, i.e. apoptotic cell condensation, nuclear fragmentation and flippase induced movement of phosphatidylserine from the inner to the outer leaflet of the plasma membrane (1, 2), blebbing in the plasma membrane, and cell shrinkage (1, 2). The apoptotic cell is then transformed into apoptotic bodies (membrane bound entities) (4).

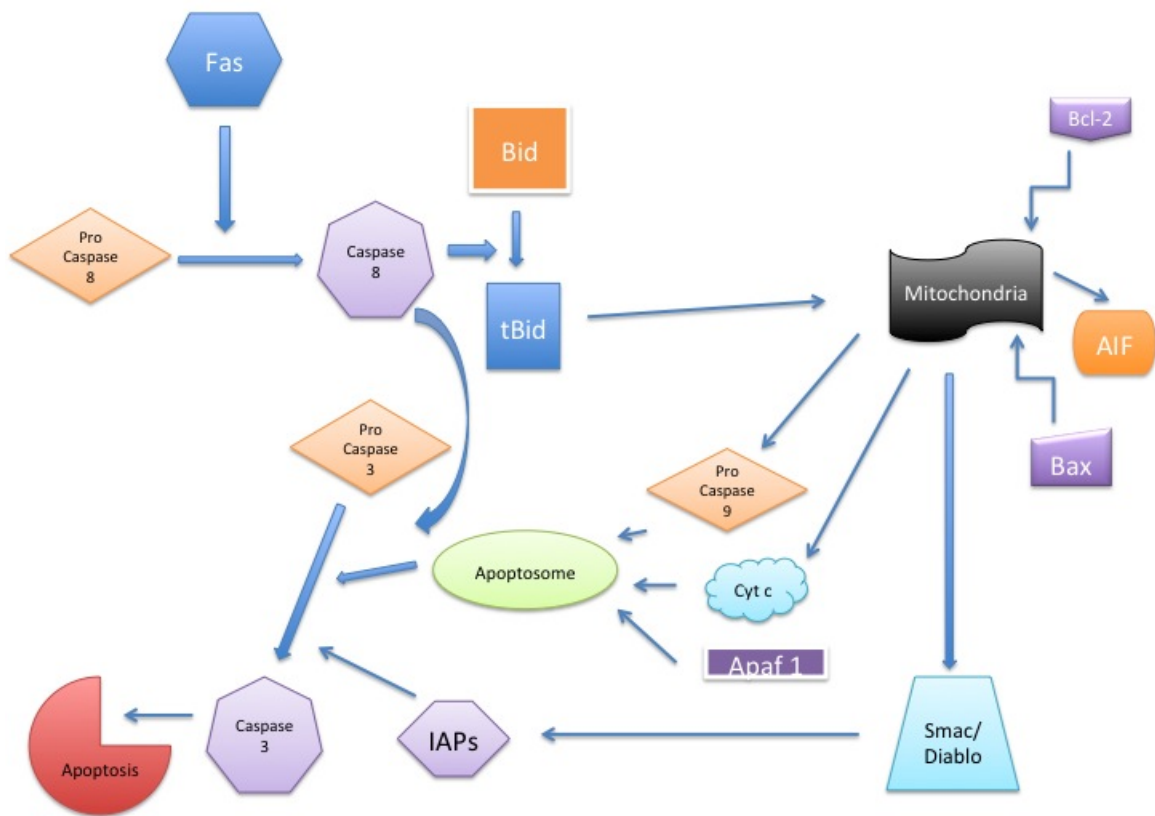


Fig.1. Schematic diagram of Mitochondria mediated apoptosis pathways

The path by which these proteins egress is subject to intense research and a number of possible pathways have been proposed/ conjectured so far. The basic reason behind the proposal of many alternate mechanisms is the conflicting evidence of their presence.

Various factors can affect the initiation of apoptosis; such as DNA damage, stress, and calcium homeostasis. Voltage Dependent Anion-selective Channel (VDAC) closure is also linked to apoptosis (5,6). Cell cycle enzymes, Bcl-2 family proteins, VDAC, Neuronal Apoptosis Inhibition Factor (NAIP) as well as Tumor Necrosis Factor (TNF) are believed to regulate cell proliferation and cell death. Interaction of Bcl-2 family proteins with mitochondria induce release of inter membrane space proteins to the cytosol, e.g. cytochrome *c*, Smac/Diablo and Apoptosis Inducing Factor (AIF).

Released cytochrome *c* then binds to Apoptosis Protease Activating Factor 1 (APAF-1), activating procaspase-9. Caspase-9 then cleaves and activates caspase-3. In this way the caspase cascade becomes fully operational. After cascade operationalization, DNases, transglutaminases and endonucleases become activated through the caspase cascade pathway, which eventually leads to the blebbing of the cell. Release of cytochrome *c* is considered to be an irreversible step in apoptosis (7), but the release should be accompanied by functional APAF-1 in order to make the cell really committed to death (8).

There are many tentative models in place, to address the egress of important IMS Proteins, necessary for the execution phase of apoptosis. One prominent model out of many existing ones is formation of lipidic pores. Bax induces some changes in membrane

monolayer, promoting a change in membrane curvature and thereby promoting the formation of a lipidic pore. This proves the role of Bax in the formation of apoptotic pores (9). Formation of channels by pro-apoptotic protein Bax is also forms integral part of models revolving around it. In apoptotic cells or when Bax is targeted to the mitochondrial membranes, bax then triggers release of cytochrome *c*, which starts downstream discrete steps of intrinsic apoptosis (10). Mitochondrial Apoptosis induced Channels (MAC) is another prominent candidate which forms apoptotic channels in mitochondria. Characteristically it is slightly cationic 2-nS conductance channel. This channel is said to be large enough for cytochrome *c* egress (11). Last but not the least Mitochondrial Permeability Transition Pore (MPT) is also a well accepted model in this field. The MPT pore is formed in the mitochondrial inner membrane resulting in mitochondrial swelling. This may lead to protein release from the intermembrane space. (12). These are some of the proposed pathways through the mitochondrial membranes and these examples are far from being exhaustive.

Experiments done previously in the laboratory of Dr. Colombini proposed one such unique mechanism, which is the formation of channels by a sphingolipid called ceramide. Ceramide is well known as a proposed second messenger. Activation of cytokine receptors results in the elevation of ceramide levels acting as a second messenger signaling molecule. Ceramide plays a role in apoptotic signaling. By analogy with diacylglycerol (DAG), ceramide has been suggested to fulfill a second-messenger

function by binding to specific intracellular protein targets.

Research from Dr. Colombini's laboratory has shown that in addition to this proposed role as a second messenger, ceramide also directly participates in permeabilization of the mitochondrial outer membrane (12). Functional studies have shown that ceramide helps in the MOM permeabilization by forming stable channels through which IMS proteins are released to cytosol, which is a significant advancement in the field of apoptosis.

This dissertation presents direct structural evidence of ceramide channel formation, unlike previous studies. Past research in this field has established the existence of ceramide channels and proposed models for their structure through modeling and by using functional data. A working model of the ceramide channel was produced and supported by molecular dynamic simulations (13) and electrophysiological experiments. However, no direct structural evidence supporting the model was available prior to the work presented here. The work presented in this thesis represents the first visualization of ceramide channels reconstituted in liposomes through the use of Transmission Electron Microscopy (TEM).

In this context, it will be useful to introduce some background on ceramide.

Ceramide:

Ceramide is a sphingolipid discovered by a German physician-biochemist Johann Thudichum in 1884. The enigmatic behavior of this lipid borrowed its name from the Sphinx of Egypt. The importance of ceramide remained undervalued for a long time after its discovery. The scenario changed when researchers started paying attention to

ceramide as a second messenger. Among many members of the sphingolipid family, ceramide is the most prominent one and plays an important role in intracellular signaling.

Intracellular vesicular transport plays an active role in signaling, and ceramide plays an important role in this process. Ceramide has a sphingosine base along with a fatty acid tail. The chain length of the acyl chain is variable, depending on the specificity of the synthetic enzyme. Ceramide's nature of spontaneous inter bilayer or trans bilayer movement and ceramide mediated signaling adds to its hydrophobic nature and insolubility in aqueous environment which permits ceramide to spend most of its life in membranous environment. As Hannun *et al.* describes, (14) stress induced ceramide level elevation provides some insight into its potential role as a second messenger. Later the increase has been associated though with ceramide channel formation. C₁₆-ceramide, or N-palmitoyl-D-erythro sphingosine (figure.2.), is one of the naturally occurring ceramides.

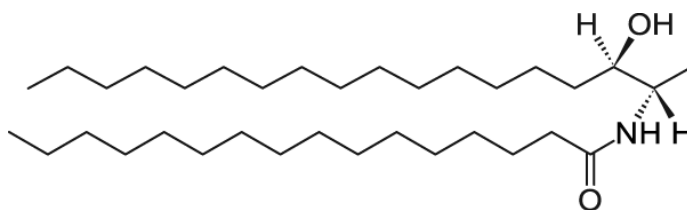


Fig.2. *N*-Palmitoyl-*D*-erythro-sphingosine (C16 ceramide)

(Source: Avanti Polar Lipids)

Activation of ceramide-dependent signaling can be caused by extracellular messages.

Ceramide metabolism is an important factor in channel formation. Ceramide molecules in a channel are in dynamic equilibrium with monomers (15) in the membrane, and thus the level of ceramide present in the MOM environment plays a very important role in channel formation. Therefore, ceramide metabolism is a key factor in ceramide-mediated apoptosis, i.e. an elevation in ceramide level due to metabolism can trigger channel formation solely due to having a high level of ceramide in the MOM environment. Thus, elevation of ceramide levels resulting from metabolism could initiate channel formation.

Ceramide transport from other organelles to mitochondria can be very important in the context of mitochondria-mediated apoptosis because it requires a significant amount of ceramide to be present in MOM in order to form a channel.

Ceramide-metabolizing enzymes are mainly found in the ER and Golgi with lesser amounts in mitochondria. The collision model of ceramide transport established by Stiban *et al.* suggests a strong possibility of ceramide transfer from ER to mitochondria via membrane-to-membrane contact (16). Long-chain ceramide transfer from ER to mitochondria is possibly a key element in permeabilizing MOM to release IMS proteins (16). In the same research article, experiments were done to understand the nature of lipid transfer from ER to mitochondria and the time dependence of the same. It was found that the above-mentioned transfer takes place in a time-dependent fashion and through close contact between the membranes of two organelles as a result of random collision. The timescale of lipid exchange suggests a rapid transfer from ER to mitochondria (17, 18).

Ceramide can be synthesized by two pathways:

- 1) De Novo pathway involving sphinganine and acyl-CoA,
- 2) Salvage pathway involving sphingomyelin.

1. De Novo pathway:

This pathway starts when the amino acid serine, reacts with fatty acyl CoA in a condensation reaction catalyzed by Serine Palmitoyl Transferase (SPT). This enzyme is a heterodimer (53 and 63 kDa subunits), bound to the ER membrane (19). This results in a product named 3-ketosphinganine, which then is used by ketosphinganine reductase to form sphinganine by a reduction reaction.

Sphinganine is in turn used as a substrate by dihydroceramide synthase to form dihydroceramide, which is a precursor of ceramide in the cell. Dihydroceramide desaturase plays an important role in ceramide-mediated apoptosis because it desaturates dihydroceramide to form ceramide(Figure.3).

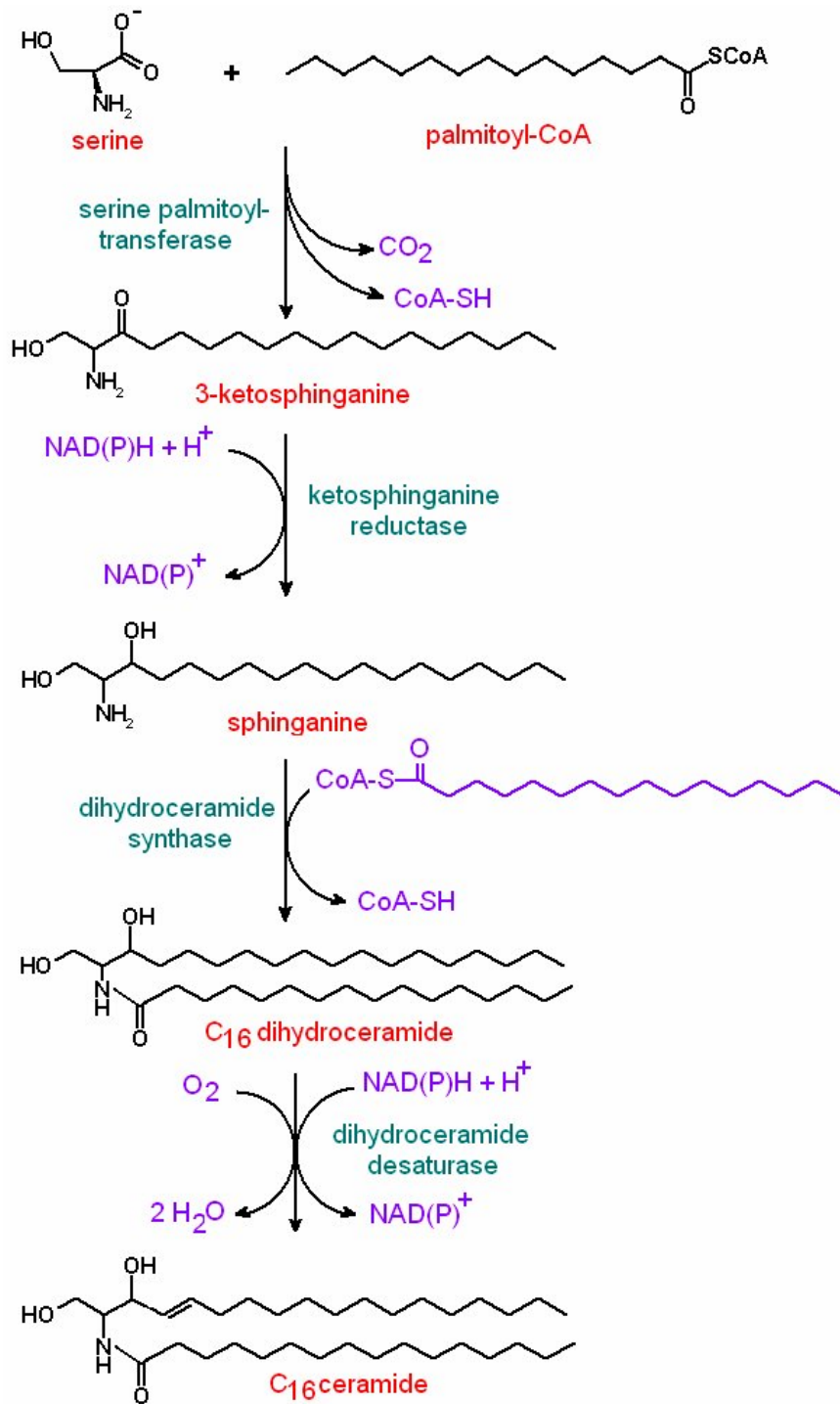


Fig.3. A schematic diagram of the *de-novo* pathway

(Courtesy: Dr Johnny Stiban)

2. Salvage Pathway:

Another way of producing ceramide in the cell is through Sphingomyelinase (SMase), which hydrolyzes sphingomyelin (Fig. 4). There are different isoforms of SMases available. Three of them are acidic and two of them are neutral in nature. Neutral ones are localized to the ER, Golgi and plasma membrane (20). The enzymes responsible for ceramide metabolism are mainly located in ER and Golgi and sometimes in mitochondria (21, 22).

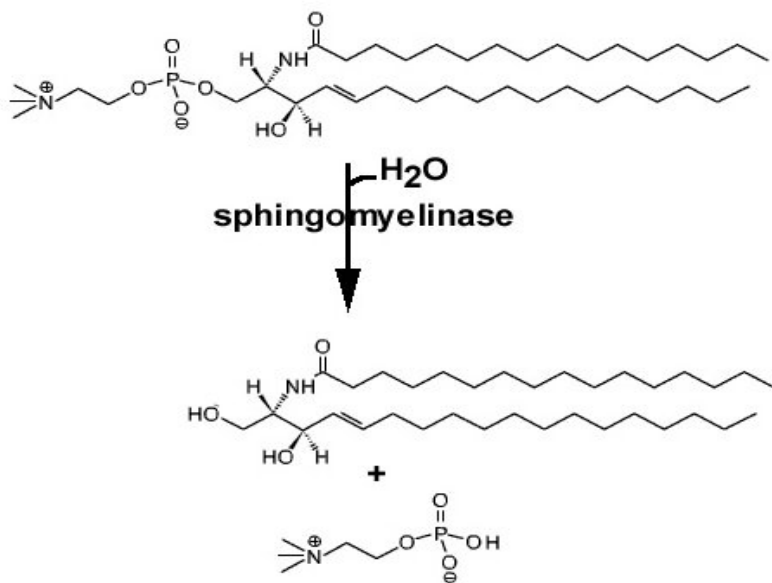


Fig.4. Sphingomyelinase transport pathway

(Courtesy: Dr Johnny Stiban)

Dihydroceramide Desaturase (DDase) is one of the critical enzymes of the *de novo* ceramide synthesis pathway. It is present only in the ER. Mitochondrial ceramide is

usually generated through the de novo pathway, which can be produced by two possible ways:

1. Presence of a mitochondrial DDase
2. Transfer of ceramide from ER to mitochondria

Ceramide Assembly:

Polar lipids are best known for self-assembly in an aqueous environment especially in the formation of a membrane. Assembly of polar lipids can occur within the lamellar phase of membrane. Ceramide is a two-tailed lipid with an 18 carbon largely aliphatic chain amide linked to a fatty acid, which is variable in length and degree of saturation. Because of the presence of ceramide's polar head groups, it also has a self-assembling capability in the membranous environment.

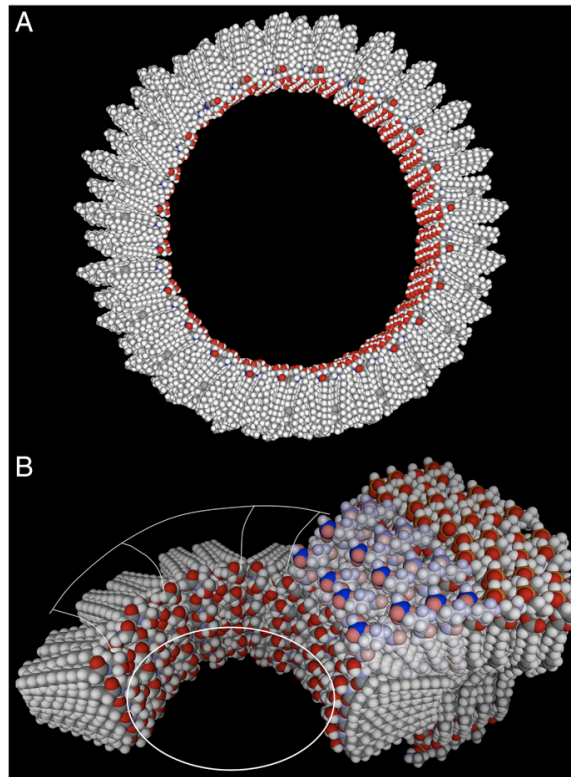


Fig. 5 Functionally derived structure of ceramide channel

The presence of a trans double bond between carbons 4 and 5 of the sphingoid base has been found to be crucial in maintaining ceramide's channel forming ability (24).

In vitro experiments performed with ceramide in a planar membrane environment and rat-liver mitochondria shows ceramide's channel forming ability. In the MOM it occurs in a dose and time dependent manner (18), which is reinforced by in vivo experiments done with whole cells (23). The ceramide channel can be large enough to let almost all IMS proteins to pass through it (18). TEM image analysis of ceramide channel reconstituted in liposome showed that the channel size in a liposome membrane environment could be as big as 50 nm in diameter. On the contrary, functional data driven diameter distributions, generated from isolated rat liver mitochondria, also suggests variability in channel diameter. The TEM data, along with functional data found in previous experiments, clearly suggest that the diameter of ceramide channels is independent of the energetics of membrane curvature. Therefore, in light of the previous statement, the roles of Bcl-2 family proteins gain prominence, which may contribute directly in ceramide channel diameter determinacy.

Studies of the disassembly of ceramide channels in the planar membrane environment show a pattern of disassembly at multiples of 4nS (14). This indicates of the disassembly of a barrel-like structure. This was consistent with a previous model of the ceramide channel where 6-ceramide molecules (based on the thickness of the

membrane) form a column connected through the amide nitrogen of one molecule with the carbonyl oxygen of another molecule. It is suggested that these columns self associate in a membranous environment in an anti parallel fashion to form a barrel-like structure. These columns work as staves of a barrel and they are connected through hydrogen bonding. The molecular dynamic simulations suggest the formation of an hourglass-like shape of the channel, which actually helps the tail region of ceramide to be completely buried into the non-polar environment of the membrane. Dipole-dipole electrostatic interactions of

ceramide columns were proposed to help stabilize the channel along with various hydrogen bonding, i.e. column remains in order by amide bonding along with cooperative tails packing. Interlayer and inter column hydrogen bonds keeps the pairs of antiparallel columns together. circular hydrogen bonding between hydroxyls and water bridges essentially keeps the staves of barrel (the column pairs) in channel (13)

The above-mentioned findings about the ceramide channel have received direct structural support by this thesis research.

Transmission Electron Microscopy:

Transmission Electron Microscopy (TEM) is a very powerful tool for imaging. It is widely used to image various samples in the field of material science i.e. to study the atomic structure of defects or to study grain boundaries. In the field of structural biology, TEM is used to study subcellular organelles and determine the ultrastructure of various biological molecules, proteins, viruses etc. In TEM, a beam of electrons is

passed through a specimen; image of the sample is formed by the interaction of the electron with the sample and then imaged on an imaging device. They have significantly higher magnification than light microscopes (26).

Light microscopes magnification is limited by the wavelength of light, which has a specific range. The formula of resolution (d) of a microscope is

$$d \approx \lambda / 2n \sin \alpha$$

Where (λ) is the wavelength of the light, (α) is numerical aperture of the lens, (n) is a

constant, changes only with the medium. Visible light has a minimum wavelength of about 400 nm. So there is a limitation of these microscopes in terms of resolution, which is a key parameter to decide the power of a microscope. Resolution of any light microscope is also affected greatly by the Numerical Aperture (NA) of the lens/ lenses of the system. In this regard TEMs have significantly higher NA, which is dynamic in nature. In TEM, the presence of a dynamic NA exists because of its virtual lenses made of electromagnetic coils, and variable diameter annular plate responsible for the aperture.

The resolution of an optical system is the ability to resolve detail in the object that is being imaged. The more powerful the microscope, the better the resolution. In case of the electron microscope, λ of electron is very small e.g. 0.005 nm (26), giving a resolution of 0.127 nm (26) Behind the high resolution of the system (TEM) lies the electron wave property. That matter shows both particle and wave properties, is well

established by the quantum mechanics. This mechanism is utilized in TEM. Release of electrons from the electron gun filament can be termed as a thermionic emission (27) or a field electron emission. In this type of emission, when a metal is heated, ion carriers like electron at the surface of the metal gain energy to overcome the binding potential of the metal, therefore those electrons free themselves from the metal surface and move away. Then the electrons are accelerated by the electric potential and focused onto samples by condenser lenses and other lenses made by electromagnets. The transmitted beam contains the phase and periodicity, which are important factors used to form an image.

For electron microscopes, the modified equation of wavelength would be

$$\lambda_e \approx h / \sqrt{2m_0E(1+(E/2m_0c^2))}$$

Because of the very low magnitude of Planck's constant (h), and very high value of the speed of light (c), the resultant wavelength (λ_e) is very small, whereas (E) defines the energy of an accelerated electron, and (m_0) defines the rest mass of an electron. (28)

Because the TEM is one of the mainstays of this thesis research, it would not be inappropriate to discuss more about transmission electron microscopy and sample preparation.

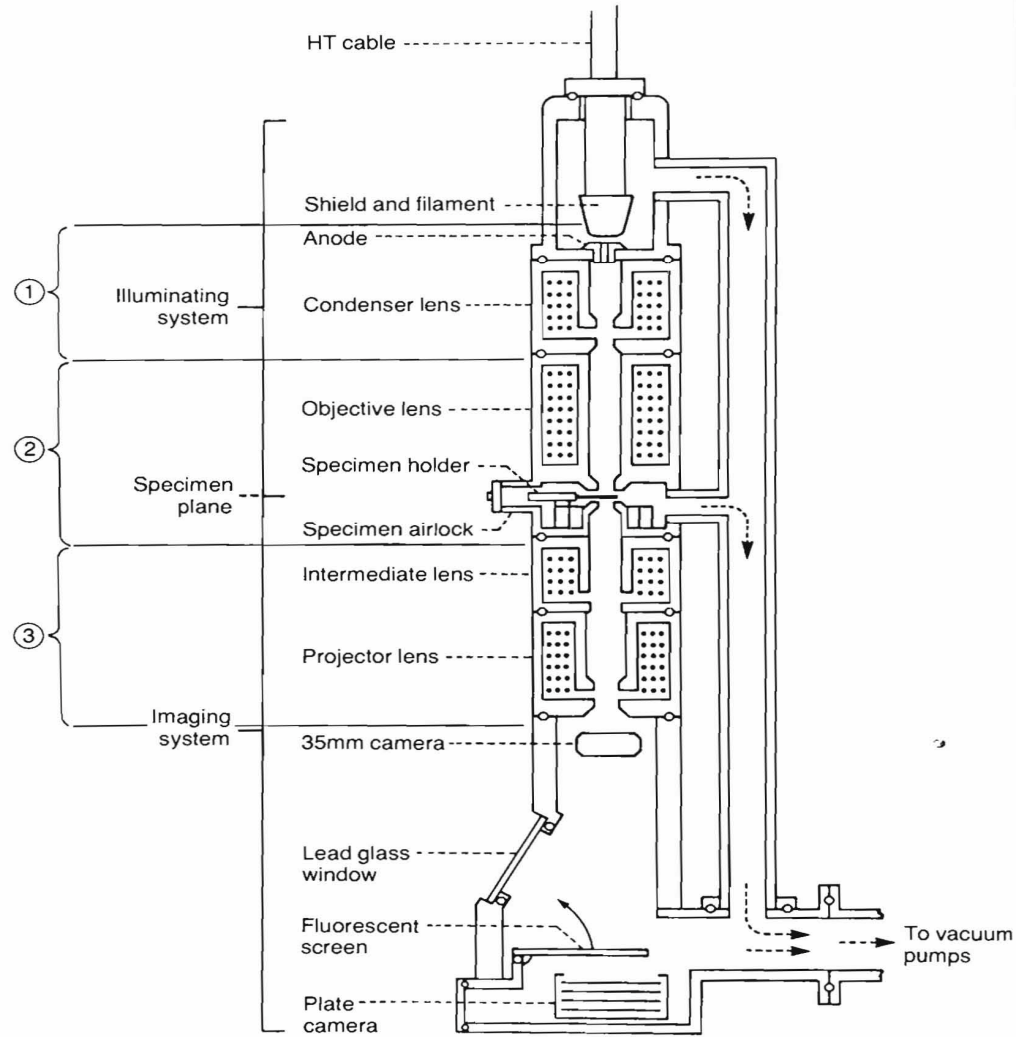


Fig.6. Schematic diagram of Transmission Electron Microscope (TEM)

(Sourced from: E. Hunter, Practical Electron Microscopy: A Beginners Illustrated

Guide, Cambridge University Press, 1993)

Electron emission source:

The electron microscope has an electron gun as a source of the electron beam. The emission source is primarily made of the filament, biasing circuit, a wehnelt cylinder. The filament emits electrons at an angle so that they can converge most of the electrons at one point. Wehnelt cylinders are designed to help the outgoing electron beams from the emission source to converge at one point and help getting directed towards condenser lenses by converging them. (27).

Electromagnetic Lenses: They emulate optical lenses. These lenses are made of a metal coil, which is used to generate magnetic or static electric fields. The widely used ones for convex lens generation are the electromagnetic ones. Through regulation of the level of current flow through these coils one can regulate the electron beam alignment, magnification etc. Radial symmetry is a very important aspect to maintain in order to get rid of various aberrations. The selection of material is also important in order to avoid hysteresis and permeability. The electron beam, generated by the electron gun then goes through various magnetic coils. Modifications of the level of current-flow through the coils produce electromagnetic fields of various strengths. These electromagnetic fields act like a magnetic condenser and aperture lenses and condense and magnify the image by regulating the electron beam in a suitable fashion. The coils allow formation of quad or hexapole magnetic lenses for beam asymmetry, called astigmatism (29).

Aperture:

Apertures are annular metallic plates. These allow the passage of electrons that are aligned through a specific axis (optic axis) mentioned and do not let other scattered electrons pass. So it is primarily a filtering mechanism.

Imaging:

Electrons wave property and periodicity carries the necessary information to form an image of the object of concern. The beam exiting from the sample has a particular amplitude which is a basic property of its wave function is proportional to the resolution of image. It's the combination of amplitude and phase that creates the image. (30)

Imaging is done on a phosphor-coated screen, usually made of zinc-sulphite. This imaging screen is coupled with a CCD cameras or film based imaging devices that capture the image.

Vacuum system of TEM:

The whole of TEM column is evacuated to minimize the collision of electrons with the air particle, which might cause partial defection of electrons from its designated path as well as the collision might produce heat. Evacuating the tunnel through which the

electron beam moves increases the mean free path of the electron particle. Another positive side of having low air pressure is avoiding an 'arc' between the top cathode and ground (31).

Specimen holder:

Specimen holder is specifically designed to hold the specimen grid rightly aligned to the electron beam. It also has an air lock system that lets the rest of the column in vacuum while allowing the filling in and evacuation of air in the holder chamber while changing samples (32).

Sample preparation:

Sample preparation is one of the key areas of transmission electron microscopy. In the method section of this thesis, I have discussed our sample preparation in detail, but here I will discuss the general sample preparation techniques for TEM. The sample is placed atop a thin carbon coated metal grid (copper generally) with a very thin plastic coating on it. Because the electron beam readily interacts with the sample placed on the grid, and basically traverses through the sample to form an image on the screen, the sample cannot be thicker than hundreds of nanometer (26). This is unlike X-ray diffraction, where diffraction is measured, and a thicker sample is considered better. So samples have to be material transparent. In case of biological samples, a fixative is necessary in order to provide rigidity to the sample structure (26). Stains have a dual role to play, first they are used as chemical fixatives, which give rigidity to biological sample

structure, and they provide the necessary contrast for transmission electron microscopy (26).

Negative Stain:

Negative stains are basically salts of heavy metals like uranium, tungsten, osmium etc. Heavy metals are useful because of their ability to deflect electrons or scatter them to other directions and deviate them from their path. Negative stain forms an amorphous glassy layer of stain on the grid surface and helps formation of a background smooth image plane. Negative stain deposits around the sample on the grid plane. Negative staining deposits heavy metal everywhere but on the sample. This phenomenon gives contrast between the background and sample, called negative contrast. Heavy metal deposition around the sample is much more than other parts of the grid, and decrease of concentration of heavy metal deposition around the sample is inversely proportional to the distance from the sample. At sample boundary, deposited amount of metal is the highest. As distance increases from the sample boundary on grid plane (moving along X axis in a XYZ coordinate system), deposition reduces in a linear fashion. Uranyl acetate, uranyl formate, phosphotungstic acid and ammonium molybdate are good examples of negative stain. Negative stain also gives rigidity to the biological samples so they do not undergo any more morphological changes after negative stain treatment, and can be preserved for months and can be seen under TEM with unaltered structure (26).

Positive Stain:

The function of positive stain is quite similar to that of negative stain in terms of giving stability to the sample and increasing contrast, but along with that, it also has a role of engaging in cross linking reaction with the unsaturated double bonds of the sample if present, and the area where this reaction occurs gets a black spot. Heavy metal salts present in a positive stain, unlike negative stain, attach to the specific samples to increase the density of the samples, increasing positive contrast. This is exactly the opposite of negative contrast (26).

In this thesis research, we chose Uranyl Acetate (UA), a negative stain over positive staining because of two reasons:

1. It had better contrast
2. The operable pH range of UA negative stain was similar to that of the sample solution.

CHAPTER 2: MATERIALS AND METHODS

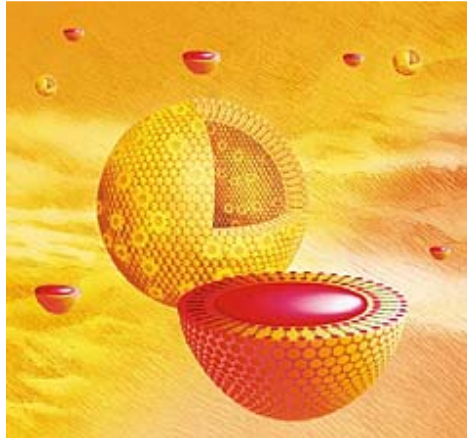
2.1 Materials:

Asolectin (a polar extract of soybean phospholipids resembling the mitochondrial outer membrane phospholipids), diphytanoyl phosphatidylcholine (DPhPC), ceramides and the materials needed for liposome formation by extrusion were bought from Avanti Polar Lipids (Alabaster AL). Formvar and carbon coated, 200 mesh copper electron microscope grids were purchased from Electron Microscopy Sciences (Hatfield, PA). DiI C12, the membrane tagging dye was bought from BD Biosciences (San Jose, CA).

2.2 Preparation of liposomes:

Liposomes were composed of asolectin: DPhPC: cholesterol in a 0.5:0.5:0.05 weight ratio. The lipids were mixed and dissolved in hexane, dried under nitrogen and placed under vacuum overnight. On occasion, the fluorescent marker DiI C12 was included at approximately a 1:50 molar ratio. The lipid was dispersed in 1 ml of 0.8M mannitol,

50mM NaCl, 10 mM HEPES, and 1mM EDTA, pH 7.2. The liposomes were sonicated and freeze thawed 4 times followed by extrusion through a 0.2 μm polycarbonate membrane for 17 passes. This last step generates unilamellar liposomes.



Cartoon of a liposome and its Interior Environment.

Figure.7. Cartoon of a liposome (Courtesy: Dr Scott Hartsel)

Formation and Separation of liposome with ceramide channel:

The basic idea behind the separation of liposomes with ceramide channel from those having no channel was to make liposome in denser buffer and then dilute them in lighter buffer having similar osmolarity, liposome with channel will float to the surface because of equilibration of buffer inside Vs. outside through ceramide channel, whereas

liposomes without channel will remain heavier and will drop to the bottom lacking equilibration of buffer inside Vs. outside.

The extruded sample (1ml) was diluted to 10 ml with 0.60M Mannitol, 0.10M NaCl, 10mM HEPES, 1mM EDTA, pH 7.2. This buffer was carefully chosen because the osmolarity of the buffer equals that of the denser mannitol buffer inside the liposome. Four hundred microliters of 1mg/ml C₁₆ ceramide in isopropanol or vehicle alone were added to the diluted liposome solution while vortexing. Dilution of the liposome sample was necessary to minimize the influence of the vehicle (isopropanol). Liposomes containing channels were separated from those lacking channels by centrifugation in a step gradient. The bottom layer, containing most of the volume, was the liposome suspension. The next layer was 1ml of 0.4M NaCl containing 10mM HEPES pH 7.2. The channel-containing liposomes were expected to collect at the interface between these solutions. Aggregated ceramide molecules (ceramide micelles) should float above the NaCl layer because their density (approximately equal to water) is less than that of both Bulk mannitol buffer and NaCl buffer solution layers. To further separate the liposomes from the ceramide aggregates, 1 ml of water was layered on top of the NaCl layer. The tubes were spun in a swinging bucket rotor at an RCF=58000 at room temperature for 4 hours. In the tube containing the liposomes treated with ceramide, most of the liposomes were located at the mannitol/ NaCl interface (Fig. 9A). The liposomes only treated with isopropanol (vehicle control) sedimented to the bottom of the centrifuge tube (Fig. 9B). Once removed from the gradient, the liposome suspension was concentrated further by placing it in a dialysis tube and adding polyvinyl pyrrolidone, with average molecular weight of 40,000, around the tube.

2.3 Transmission electron microscopy:

Carbon coated formvar grids were used for the study. The grid was floated on top of a drop of sample for fifteen minutes followed by floating on top of osmium tetroxide (2% aqueous solution) for ten minutes. Then it was floated on top of 1% aqueous uranyl acetate for 1 min and after air-drying, it was observed under TEM. The electron microscopic analysis of the sample was performed with a ZEISS EM 10 CATEM at magnifications ranging from 25K – 200K. The electron micrographs were 2D projections of the negatively stained channels. Approximately equal numbers of ceramide-treated and control liposomes, treated only with the vehicle, isopropanol, were observed. No channel-like structures were ever observed on the control liposomes whereas a total of over 80 channel-like structures were observed on the ceramide-treated liposomes over many separate experiments by two investigators working independently (JS and SS).

2.4 Image analysis:

All image analysis was performed using Image J software (developed at NIH and freely available on line) at 8-bit resolution. Channel diameters were determined by densitometric slicing through the channel and measuring the distance at the inflection points. The channels were essentially circular and considering the wide variation in channel sizes, increased precision was considered to be unnecessary. Surface plots of ceramide channels embedded in liposomes were performed after inverting the image so

that dark areas appear raised. This allowed better visualization of the channel and its comparison to the depth of stain accumulated around the vesicle. The resolution of the electron micrographs, as influenced by the degree of defocusing, was determined from the first zero of the phase contrast transfer function in the Fourier transform power spectrum of a background region of the micrograph and used without further correction.

In order to test the possibility that the walls of the channels might be tilted, the density function of the cross-section at the edge of a channel was compared to a theoretical right-angled edge that was smoothed (low-pass filtered) by a moving average. To avoid sampling error, the shape of the tilt used for each channel was an average of the density function of 6 cross-sections through the channel at angles evenly spaced around the circle. The number of nanometers in the moving average was the same as the resolution determined from the phase contrast transfer function of the background. In addition, a random sample of 15 micrographs was selected and of these 13 was of sufficient quality to be analyzed further. The smoothing procedure was performed with a variable moving average and the best fit (by least squares) yielded the resolution estimate (i.e. the number of nanometers in the moving average). This value was compared to the value obtained from analysis of the background.

2.5 Electrophysiological recordings:

The formation of ceramide channels was monitored by recording the current flowing through a planar phospholipid membrane made by the monolayer technique [33] as modified [34]. The lipids used to form the membrane were DPhPC, asolectin, cholesterol, 1:1:0.2 (w/w/w). Membranes were 0.05–0.1 mm in diameter. The voltage

was clamped and the current recorded. The aqueous solution contained 100 mM KCl, 5 mM MgCl₂, 5 mM PIPES (pH 6.9) for C2-ceramide and 1.0 M KCl, 5 mM MgCl₂, 5 mM PIPES (pH 6.9) for C16-ceramide. All the experiments were performed at room temperature (about 23 °C). Ceramide was generally added to both sides of the membrane. C2-ceramide was dissolved in DMSO and C16-ceramide in isopropanol. Solutions of 0.1 or 1.0 mg/ml were used. Aliquots of 2–20 µL were stirred into 5 ml of aqueous buffer bathing the membrane. Multiple additions were often needed to achieve a substantial conductance. The dispersal of ceramide close to the membrane was essential to achieve a good conductance level with the 8 long-chain ceramide.

CHAPTER 3. RESULTS AND DISCUSSION

3.1 Generation of liposomes containing channels

Unilamellar phospholipid/cholesterol liposomes were formed by the extrusion technique. C₁₆-ceramide dissolved in isopropanol was added while vortexing to form channels in the liposomes. The amount of isopropanol was kept below 4% to avoid disturbing the liposomal membranes. This technique was shown to form channels capable of permeabilizing the liposomes to carboxyfluorescein and the permeability could be influenced by agents that influence ceramide channels [13]. The liposomes with channels were separated from those without channels and from ceramide micelles by means of a density step gradient. This took advantage of the difference in permeability of the membranes of liposomes containing channels and thus also served as evidence of channel formation. In Fig. 9A, the top of the gradient reveals the ceramide-containing liposomes as cloudy layer just below the air-water interface. There is no visible pellet on the bottom of the tube. In Fig. 9B, the top of the gradient shows no visible liposomes whereas the bottom of the tube has an evident pink pellet of liposomes containing the tagging dye.

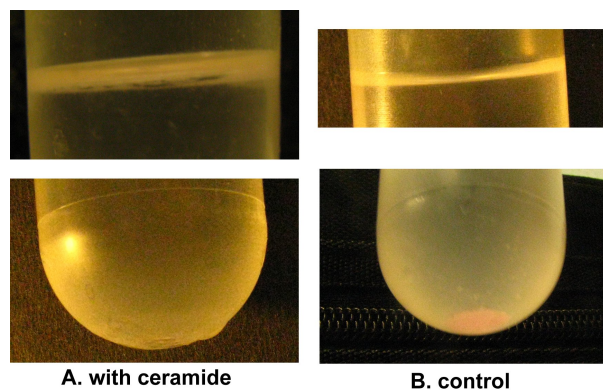


Figure.8. Location of liposomes with channel and without channel in density gradient centrifugation [A. top: Liposome with channel, bottom: no liposome] [B. top: aggregated ceramide, bottom: liposomes treated with isopropanol]

3.2 Visualization of channels by electron microscopy

Both the isopropanol (vehicle control) and ceramide treated liposomes were fixed with osmium tetroxide and negatively stained with uranyl acetate prior to observation by TEM. It is known that ceramide channels are in dynamic equilibrium with monomers or non-channel aggregates in the membrane [35-42] and thus osmium tetroxide was used as a mild fixative to stabilize the channels. The osmium tetroxide treatment alone produced little staining. The subsequent treatment with uranyl acetate visualized the channels. As a negative stain, uranyl acetate forms an amorphous, glassy layer that fills spaces, such as channel lumens, causing these to be electron opaque. Some of the ceramide-treated liposomes had black circular structures (Fig. 10), interpreted as stain-filled cylindrical channels.

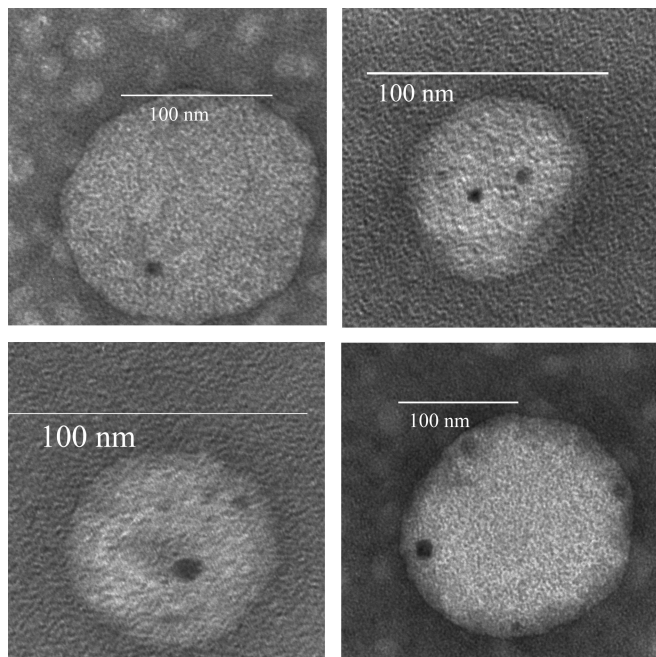


Figure.9. Liposomes with ceramide treatment having channels

A total of over 80 channel-like structures were observed on the ceramide-treated liposomes over many separate experiments by two investigators working independently (JS and SS). A similar number of isopropanol treated liposomes (Fig. 11) were observed as those treated with ceramide yet none of these control liposomes had the structures seen in the ceramide-treated liposomes, demonstrating that the channel-like structures were induced or produced by ceramide.

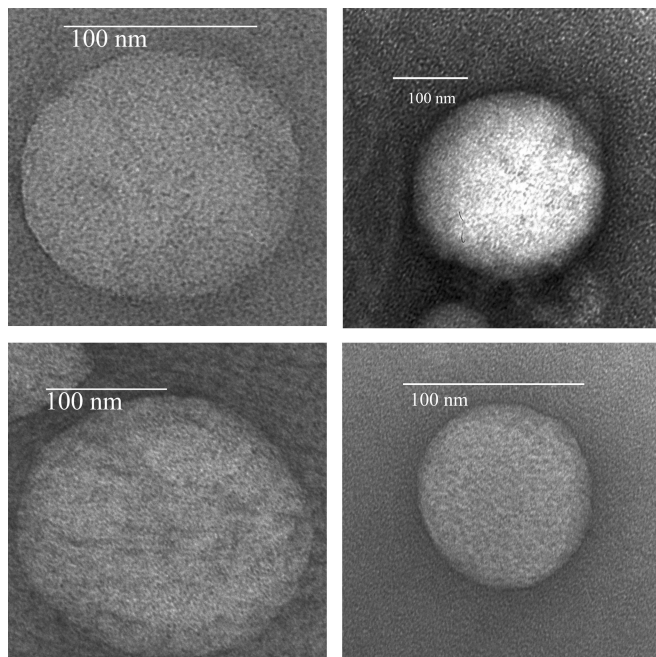


Figure.10. Liposomes with control (vehicle) treatment

Dihydroceramide-treated liposomes were indistinguishable from controls. This is expected because dihydroceramide does not form channels in mitochondria [24], planar membranes [26, 36] or liposomes [24].

A histogram of the diameters of the circular channel-like structures shows a size range from 5-38 nm (Fig. 12). The resolution limit for negative staining is 1.5-2 nm [27] and thus these structures are well within the scope of the method. However, smaller channels may have been present and not detected because of the limitations of the method.

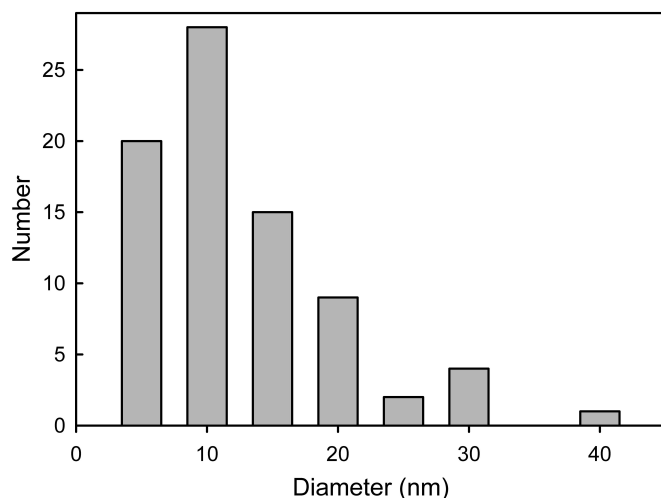


Figure.11. Histogram of channel diameters

The amorphous, glassy nature of the negative stain allowed us to distinguish between a surface feature and a channel with depth. As the stain dries over and around the flattened liposome, the stain can accumulate at the edge and its thickness can decline with distance from the liposome in an exponential fashion (Fig. 13A) or the vesicle can displace stain from a fairly even background (Fig. 13B). The gray scale of the scanned image has 8-bit resolution and represents the quantitation of the electron micrograph. The gray scale values should be proportional to the thickness of deposited stain because the heavy metals in the stain are the major electron scatterers and the greater the amount of stain the fewer electrons will hit the photographic negative. The major peaks within this outline of the vesicles in Fig. 13 are the stain-filled channels. The accumulation of stain within the channel results in a gray scale that is comparable with the accumulation of stain around the flattened vesicle showing that what we interpret as channels have significant depth and thus are unlikely to be minor surface indentations.

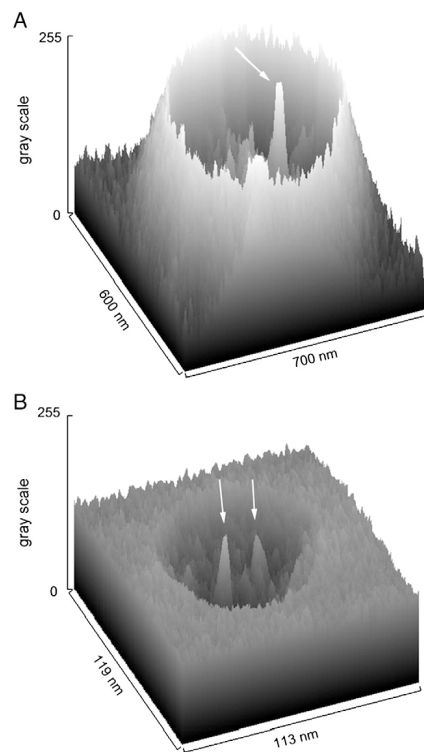


Figure.12. Surface plots of the stain density of electron micrographs of vesicles containing one (A) and two (B) channels. The gray scale was inverted so that the highest value has the darkest stain. Arrows indicate the location of the stain-filled channels

The cross-sectional view of the stain density of the stain-filled channels is not rectangular but rhomboid in shape. This is expected because the image is blurred by the contrast transfer function of the microscope. However, one can ask whether the shape is within the limits expected for a cylindrical channel or perhaps indicates the formation of something other than a right cylinder. For instance, the channel might have tilted sides, forming a truncated cone. To look for evidence of deviations from a right cylinder, we compared the density function of the cross-section at the edge of a channel to a theoretical right-angled edge that was smoothed (low-pass filtered) by a moving average. In the two examples shown in Fig. 13, the degree of smoothing was

determined by the resolution estimate determined from the first zero of the phase contrast transfer function (CTF) of the Fourier transform power spectrum of a background region of the same electron micrograph from which the image was obtained (1.25 nm for panel A and 1.0 nm for panel B of Fig. 13).

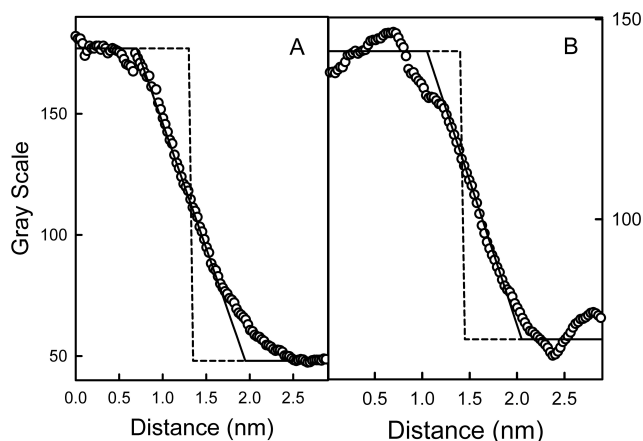


Figure.13. Expected tilt of channel edge compared to experimental data

In these cases the agreement between experimental results and theoretical expectation can be seen visually to be very high. Alternatively, smoothening of the theoretical right-angled edge was varied until it gave a best fit to the density function cross-section of the micrograph of a channel and from this an apparent resolution was obtained that could be compared to that determined from the CTF of the background. This was done by sampling 13 micrographs. The average resolution from the fits was 1.3 ± 0.3 and that from the CTF was 1.4 ± 0.3 . The average of the differences was 0.12 nm, only 10% of the value of the resolutions. Thus, the observations are consistent with a channel forming a pore that is a right cylinder. More sophisticated methods will be needed to rigorously explore the shape of the channel.

Planar membrane data also agreed with TEM experiment derived results and confirmed the size distribution and structure of the ceramide channel.

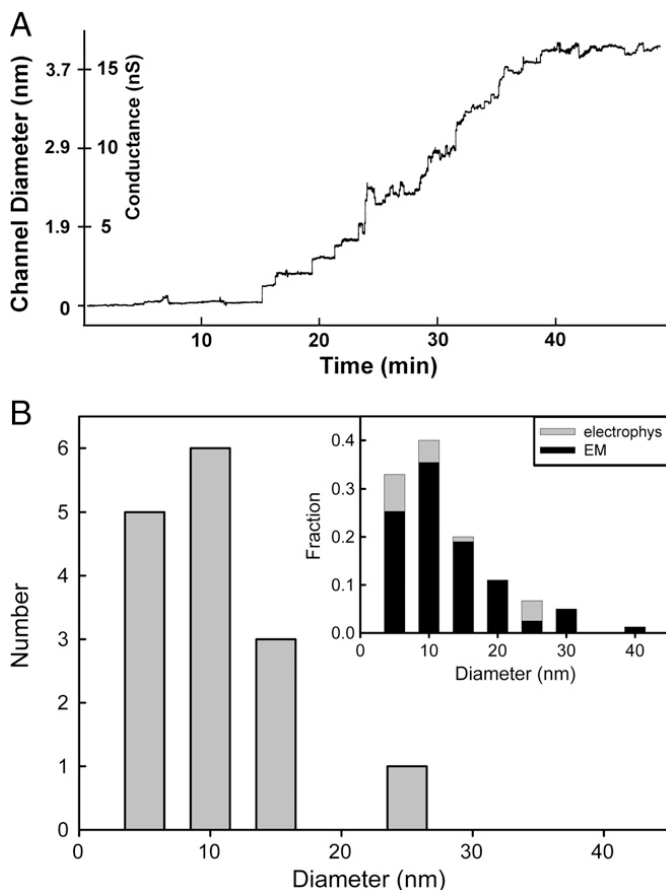


Fig. 14. Sizes of ceramide channels measured from electrophysiological experiments. (A) A typical trace of conductance increments in a planar phospholipid bilayer following the addition of C16-ceramide to the aqueous compartment. This is the growth of a single ceramide channel [15]. The calculated channel diameter is also indicated on the y-axis. (B) Histogram of the calculated size of ceramide channels from many experiments such as the one illustrated in (A). In the inset, the number of events is expressed as a fraction of the total number of events and the results from electron microscopy (EM) and electrophysiological recordings are plotted together for comparison.

The planar membrane experiments are another way to measure the size of ceramide channels. These sizes can be compared to the sizes determined by TEM. Ceramide is

known to form large and stable channels in planar membrane [25,43]. Addition of ceramide to phospholipid membranes results in conductance increments that culminate into a final steady-state conductance (Fig. 14A). In most cases, this final conductance has been shown to be due to a single gargantuan channel [15]. Due to the large size of these channels, one can calculate their diameter with high accuracy knowing the conductance of a cylinder of solution and the access resistance of the medium.

$$d = \sqrt{\frac{4\rho L G}{\pi G^2 + 4\rho L G}}$$

Where d is the diameter of the pore, G is the measured conductance, ρ is the resistivity of the medium (8.94 Ω cm for 1.0 M KCl), L is the length of the channel (taken as 5 nm) and π has the usual value. The length of the channel was assumed to be 5 nm. Separate histograms of channel diameter sizes calculated from TEM and planar membrane experiment data (Figs. 11 and 14B, respectively) show a virtually identical distribution. Both data sets were converted to fractions of the total number of observations and plotted together in the inset to Fig. 14B for easy comparison. Both histograms are asymmetric, with long tails on the side of large channels. This indicates that the channel sizes are not clearly limited. Electrophysiological measurements have recorded channels with much larger calculated diameters.

4. Conclusion:

This work presents the first visualization of the large channels formed by ceramide in phospholipid membranes. Channel sizes peak around 10 nm but do not show a normal distribution, indicating that the size is not strictly limited by the energetics of channel curvature. Indeed, both the TEM and functional studies show that the channels can achieve very large sizes. The size may be restrained in mitochondria by Bcl-2 family proteins as previously reported [44]. The ability to form very large channels is in agreement with models of the ceramide channel structure deduced from functional studies [43] and supported by molecular dynamics simulations [13]. The large channel size is also in agreement with all the inter membrane space proteins that are released on the onset of the induction phase of apoptosis. These results may not apply to other structural forms of ceramide, such as skin ceramide that has been shown [45] to act by changing the overall morphology of liposomes.

References:

1. Jacobson, M.D., J.F. Burne, M.P. King, T. Miyashita, J.C. Reed, and M.C. Raff. 1993. Bcl-2 blocks apoptosis in cells lacking mitochondrial DNA. *Nature* 361:365-369.
2. Jacobson, M.D., J.F. Burne, and M.C. Raff. 1994. Programmed cell death and Bcl-2 protection in the absence of nucleus. *EMBO J.* 13:1899-1910
3. SR Wiley, K Schooley and PJ Smolak *et al.*, Identification and characterization of a new member of the TNF family that induces apoptosis, *Immunity* 3 1995, pp. 673–682
4. Wyllie, A.H., J.F.R. Kerr, and A.R. Currie. 1980. Cell death: the significance of Apoptosis. *Int. Rev. Cytol.* 68:251-306, 1980
5. Lai, J.C., W. Tan, L. Benimetskaya, P. Miller, M. Colombini, and C.A. Stein. 2006. A pharmacologic target of G3139 in melanoma cells may be the mitochondrial VDAC. *Proc. Natl. Acad. Sci. U S A.* 103(19): 7494-7499.
6. Tan, W., J.C. Lai, C.A. Stein, and M. Colombini. 2007. Phosphorothioate nucleotides reduce mitochondrial outer membrane permeability to ADP. *Am. J. Physiol. Cell Physiol.* 292(4): 1388-1397.
7. Susin, S.A., N. Larochette, M. Geuskens, and G. Kroemer. 2000. Purification of mitochondria for apoptosis assays. *Methods Enzymol.* 322:205-208
8. Sanchis, D., M. Mayorga, M. Ballester, and J.X. Comella. 2003. Lack of Apaf-1 expression confers resistance to cytochrome c-driven apoptosis in cardiomyocytes. *Cell Death Diff.* 10:977-986
9. Basañez, G., A. Nechushtan, O. Drozhinin, A. Chanturiya, E. Choe, S. Tutt, K.A. Wood, Y.-T. Hsu, J. Zimmerberg, and R.J. Youle. 1999. Bax, but not Bcl-XL, decreases the lifetime of planar phospholipid bilayer membranes at subnanomolar concentrations. *Proc. Natl. Acad. Sci. USA.* 96:5492-5497
10. Antonsson, B., S. Montessuit, B. Lauper, R. Eskes, and J.C. Martinou. 2000. Bax oligomerization is required for channel-forming activity in liposomes and to trigger cytochrome c release from mitochondria. *Biochem. J.* 345:271-278
11. Guihard, G., G. Bellot, C. Moreau, G. Pradal, N. Ferry, R. Thomy, P. Fichet, K. Meflah, and F.M. Vallette. 2004. The mitochondrial apoptosis-induced channel (MAC) corresponds to a late apoptotic event. *J. Biol. Chem.* 279(45): 46542-46550
12. Crompton, M. 1999. The mitochondrial permeability transition pore and its role in

cell death. *Biochem. J.* 341: 233-249

13. Anishkin, A., S. Sukharev, and M. Colombini. 2006. Searching for the molecular arrangement of transmembrane ceramide channels. *Biophys. J.* 90(7): 2414-2426

14. Hannun, Y.A., C. Luberto. 2000. Ceramide in the eukaryotic stress response, *Trends in cell Biology.* 10(2):73-80

15. Daum, G., and J. E. Vance. 1997. Import of lipids into mitochondria. *Prog. Lipid Res.* 36: 103–130

16. Voelker, D. R. 2005. Bridging gaps in phospholipid transport. *Trends Biochem. Sci.* 30: 396–404

17. Siskind, L.J., R.N. Kolesnick, and M. Colombini. 2002. Ceramide channels increase the permeability of the mitochondrial outer membrane to small proteins. *J. Biol. Chem.* 277(30):26796-26803

18. Stiban, J., L. Caputo, and M.Colombini. 2007. Ceramide synthesis in the endoplasmic reticulum can permeabilize mitochondria to pro apoptotic proteins. *J.Lipid.Res.* 49(3):625-34

19. Hanada, K. 2003. Serine palmitoyltransferase, a key enzyme of sphingolipid metabolism. *Biochim. Biophys. Acta.* 1632(1-3): 16-30.

20. Clarke, C. J. and Y. A. Hannun. 2006. Neutral sphingomyelinases and nSMase2: Bridging the gaps. *Biochim. Biophys. Acta.* 1758(12):1893-901

21. El Bawab, S., P. Roddy, T. Qian, A. Bielawska, J.J. Lemasters, and Y.A. Hannun. 2000. Molecular cloning and characterization of a human mitochondrial ceramidase. *J. Biol.Chem.* 275: 21508–21513

22. Bionda, C., J. Portoukalian, D. Schmitt, C. Rodriguez-Lafrasse, and D. Ardail. 2004. Subcellular compartmentalization of ceramide metabolism: MAM mitochondria-associated membrane and/or mitochondria? *Biochem. J.* 382(2): 527-533.

23. Zamzami, N., P. Marchetti, M. Castedo, D. Decaudin, A. Macho, T. Hirsch, S.A. Susin, P.X. Petit, B. Mignotte, and G. Kroemer. 1995. Sequential reduction of mitochondrial transmembrane potential and generation of reactive oxygen species in early programmed cell death. *J. Exp. Med.* 182:367-377

24. Stiban, J., D. Fister., M.Colombini. 2006. Dihydroceramide hinders ceramide channel formation. *Apoptosis.*11(5):773-80

25. L.J. Siskind, M. Colombini. 2000 . The lipids C2- and C16-ceramide form large stable channels. Implications for apoptosis, *J. Biol. Chem.* 275:38640-38644.
26. A.B. Maunsbach, B.A. Afzelius, Biomedical electron microscopy: illustrated methods & interpretations, *Academic Press*, 1999
27. Buckingham, J .1965. "Thermionic emission properties of a lanthanum hexaboride/rhenium cathode". *British Journal of Applied Physics* 16: 1821
28. Champness, P. E. Electron Diffraction in the Transmission Electron Microscope, *Garland Science*, 2001.
29. Edited by Jon Orloff .1997.. Orloff, J. ed. *Handbook of Electron Optics*. CRC-press
30. Cowley, J. M. 1995. *Diffraction physics*. Elsevier Science B. V..
31. Chapman, S. K. 1986. *Maintaining and Monitoring the Transmission Electron Microscope*. Royal Microscopical Society Microscopy Handbooks. 08. Oxford University Press
32. Pulokas, J; Green, C; Kisseberth, N; Potter, CS; Carragher, B .1999. Improving the Positional Accuracy of the Goniometer on the Philips CM Series TEM. *Journal of Structural Biology* **128** (3): 250–256
- 33.M.Montal, P.Mueller .1972. Formation of bimolecularmembranes from lipid monolayers and a study of their electrical properties, *Proc. Natl Acad. Sci. USA* 69:3561–3566.
34. M. Colombini. 1987.Characterization of channels isolated from plant mitochondria, *Methods Enzymol.* 148:465–475
35. Futerman, A.H. 2006. Intracellular trafficking of sphingolipids: Relationship to biosynthesis. *Biochim. Biophys. Acta.*2006. 1758(12)1885-92
36. R.L. Thomas, C.M. Matsko, M.T. Lotze, A.A. Amoscato. 1999. Mass spectrometric identification of increased C16 ceramide levels during apoptosis, *J. Biol. Chem.* 274 30580-30588.
- 37 D. Ardail, M. Maalouf, A. Boivin, O. Chapet, J. Bodennec, R. Rousson, C. Rodriguez-Lafrasse. 2009. Diversity and complexity of ceramide generation after exposure of jurkat leukemia cells to irradiation. *Int. J. Radiat. Oncol. Biol. Phys.* 73; 1211-1218.

38. H. Birbes, C. Luberto, Y.T. Hsu, S. El Bawab, Y.A. Hannun, L.M. Obeid. 2005. A mitochondrial pool of sphingomyelin is involved in TNF α -induced Bax translocation to mitochondria, *Biochem. J.* 386:445-451.
39. Q. Dai, J. Liu, J. Chen, D. Durrant, T.M. McIntyre, R.M. Lee. 2004. Mitochondrial ceramide increases in UV-irradiated HeLa cells and is mainly derived from hydrolysis of sphingomyelin, *Oncogene* 23:3650-3658.
40. C. Garcia-Ruiz, A. Colell, M. Mari, A. Morales, J.C. Fernandez-Checa. 1997. Direct effect of ceramide on the mitochondrial electron transport chain leads to generation of reactive oxygen species. Role of mitochondrial glutathione, *J. Biol. Chem.* 272:11369-11377.
41. C.M. Matsko, O.C. Hunter, H. Rabinowich, M.T. Lotze, A.A. Amoscato. 2001. Mitochondrial lipid alterations during Fas- and radiation-induced apoptosis, *Biochem. Biophys. Res. Commun.* 287:1112-1120.
42. L.J. Siskind, R.N. Kolesnick, M. Colombini. 2006. Ceramide forms channels in mitochondrial outer membranes at physiologically relevant concentrations, *Mitochondrion* 6:118-125.
43. L.J. Siskind, A. Davoody, N. Lewin, S. Marshall, M. Colombini. 2003. Enlargement and contracture of C2-ceramide channels, *Biophys. J.* 85:1560-1575.
44. L.J. Siskind, L. Feinstein, T. Yu, J.S. Davis, D. Jones, J. Choi, J.E. Zuckerman, W. Tan, R.B. Hill, J.M. Hardwick, M. Colombini. 2008. Anti-apoptotic Bcl-2 family proteins disassemble ceramide channels, *J. Biol. Chem.* 283:6622-6630.
45. Xu. P, G. Tan, J. Zhou, J. He, L.B. Lawson, G.L. McPherson, V.T. John. 2009. Undulating tubular liposomes through incorporation of a synthetic skin ceramide into phospholipid bilayers, *Langmuir* 25:10422-10425